



Synthesis, characterization, and molecular docking of benzodiazepines in the presence of SrFe₁₂O₁₉ magnetic nanocatalyst

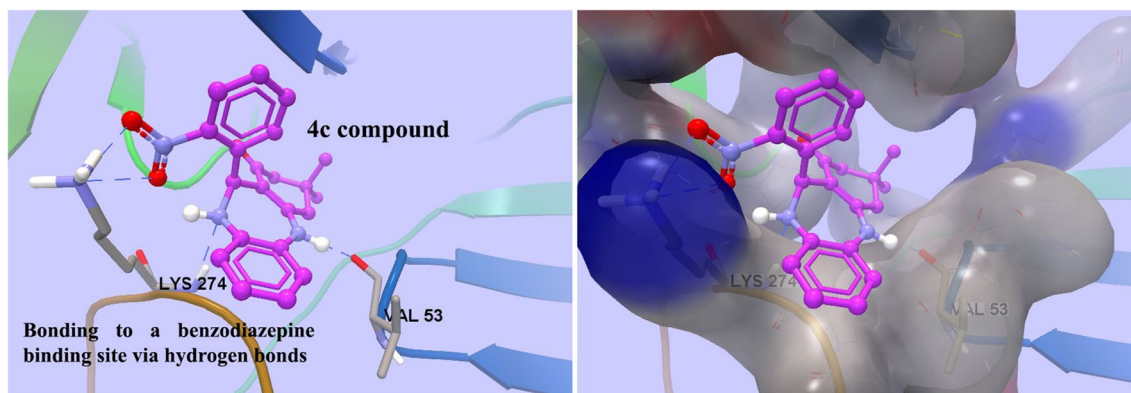
Tahereh Ahmadi¹ · Ghodsi Mohammadi Ziarani¹ · Seyed Mohsen Masoumian Hoseini² · Alireza Badiei³ · Mohammad Mehdi Ranjbar⁴

Received: 26 August 2020 / Accepted: 2 January 2021
© Iranian Chemical Society 2021

Abstract

An efficient and concise method for the synthesis of 1,5-benzodiazepine derivatives was developed using *o*-phenylenediamine derivatives, 4,4-dimethyl cyclohexane-1,3-dione, and different aldehydes through a rapid three-component domino reaction in the presence of the SrFe₁₂O₁₉ magnetic nanocatalyst under solvent-free conditions. The SrFe₁₂O₁₉ nanoparticles were synthesized using the sol-gel auto-combustion technique. The main advantages of using this nanocatalyst are its easy handling and removal from the reaction mixture, by the use of an external magnet, and reusing it several times without any loss of activity. Some parameters such as the bond length and bond strength between the obtained products and the GABA receptor were evaluated to have an insight on the interactions involved. The electrostatic energy, ligand efficiency, log P, and the total binding energy of the compounds with the receptor were also calculated.

Graphic abstract



Keywords Domino reaction · 1,5-Benzodiazepine derivatives · Nanomagneticcatalyst · Docking study · GABA receptor

✉ Ghodsi Mohammadi Ziarani
gmohammadi@alzahra.ac.ir

¹ Department of Chemistry, Alzahra University, Vanak Square, P.O. Box 1993893973, Tehran, Iran

² Clinical Biochemistry, School of Nursing, Torbat Jam University of Medical Sciences, Torbat Jam, Iran

³ School of Chemistry, College of Science, University of Tehran, 14155-6455 Tehran, Iran

⁴ Razi Vaccine and Serum Research Institute, Agricultural Research, Education and Extension Organization, Karaj, Iran

Introduction

Benzodiazepines and their derivatives have been known as an important class of heterocyclic compounds because of their diverse therapeutic and pharmacological properties. They are a group of sedative/hypnotic agents which have been introduced to clinical practice over 50 years ago [1]. In addition to their applications on medicinal chemistry,

benzodiazepines have been used as anticoagulant [2], anti-inflammatory [3], antiepileptic [4, 5], antibacterial [6], antidepressant [7], and analgesic agents [8]. Different methods have been reported for the synthesis of benzodiazepines and their derivatives. For instance, 1,5-benzodiazepine derivatives can be synthesized by the condensation reactions of *o*-phenylenediamine with α,β -unsaturated carbonyl compounds [9], -haloketones [10], and various aldehydes [11–17]. Furthermore, the synthesis of 1,5-benzodiazepines has been reported in the presence of different catalysts, such as polyphosphoric acid [18], $\text{BF}_3 \cdot \text{Et}_2\text{O}$ [19], NaBH_4 [20], CF_3COOH /dehydroacetic acid (DHA) [21], ceric ammonium nitrate (CAN) [22], $[\text{H} - \text{NMP}][\text{HSO}_4]$ as a Bronsted acidic ionic liquid [23], $\text{CeCl}_3 \cdot 7\text{H}_2\text{O}/\text{NaI}$ supported on silica gel [24], ZnCl_2 [25], $\text{SiO}_2/\text{ZnCl}_2$ [26], Fe_3O_4 nanoparticles [27], $\text{SiO}_2\text{-H}_2\text{SO}_4$ under microwave irradiation [28], ZnS [29], acetic acid under microwave irradiation [30], and MgO/POCl_3 under solvent-free conditions [31].

In this work, in the continuation of our researches [32, 33], we developed an efficient and rapid method for the synthesis of 1,5-benzodiazepines by the reaction of *o*-phenylenediamine, 4,4-dimethyl cyclohexane-1,3-dione, and various aldehydes in the presence of the synthesized $\text{SrFe}_{12}\text{O}_{19}$ magnetic nanocatalyst under green solvent-free conditions.

Experimental

Materials and methods

All the chemicals were obtained from Merck Company and used without further purification. The melting points were measured by the capillary tube method with an Electrothermal 9200 apparatus. Infrared (IR) spectra were recorded on a Fourier-transform (FT)-IR Bruker Tensor 27 instrument. ^1H NMR (250 MHz) and ^{13}C NMR (62.9 MHz) spectra were run on a Bruker DPX using tetramethylsilane (TMS) as the internal standard in CDCl_3 and DMSO. Mass spectrometry (MS) analysis was performed on a model 5973 mass selective detector (Agilent). The X-ray powder diffraction (XRD) data of the prepared $\text{SrFe}_{12}\text{O}_{19}$ nanoparticles were collected by a Philips X'pert MPD diffractometer using the $\text{Cu K}\alpha$ radiation source ($\lambda = 0.15478$ nm). The scanning electron microscopy (SEM) image was taken with SEM (MV2300).

Synthesis of $\text{SrFe}_{12}\text{O}_{19}$ nanoparticles

The $\text{SrFe}_{12}\text{O}_{19}$ magnetic nanoparticles were synthesized according to previous reports [33–38]. Briefly, the $\text{Fe}(\text{NO}_3)_3 \cdot 9\text{H}_2\text{O}$ and $\text{Sr}(\text{NO}_3)_2$ powders ($\text{Fe}/\text{Sr} = 10$) were

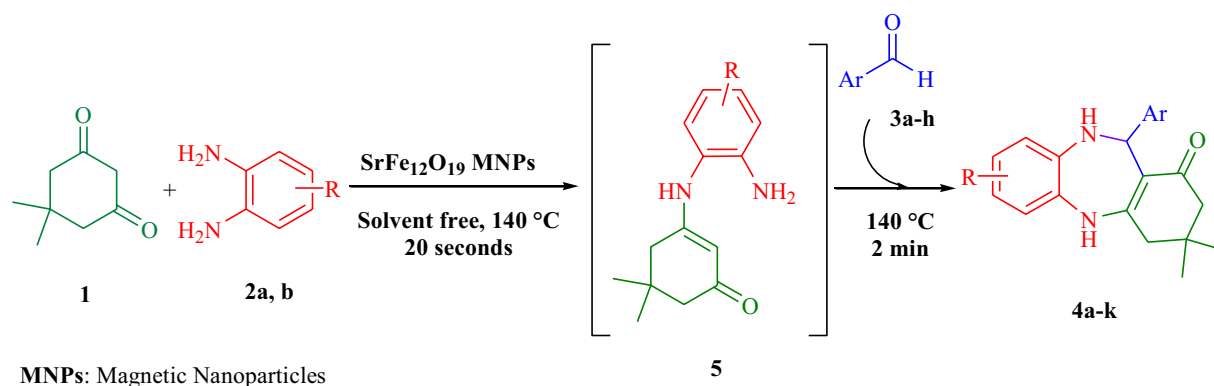
dissolved in deionized water (100 mL for 0.1 mol of Fe^{3+}) and stirred well at 60 °C to afford a clear solution. The citric acid, in an appropriate molar ratio to the used metal nitrates, was then added to the clear solution and stirred vigorously. Then, NH_4OH was added dropwise to adjust the pH to 7, and then a cationic surfactant (surfactant/strontium = 0.4) was added to the solution. Finally, the viscous brown gel produced after the evaporation of the solvent was calcined at 900 °C for 1 h.

General procedure for the synthesis of 4-substituted-1,5-benzodiazepines (4a–j)

At first, the $\text{SrFe}_{12}\text{O}_{19}$ (0.02 g) was dried in a round-bottomed flask containing a magnetic stirrer at 100 °C. The mixture of the 4,4-dimethyl cyclohexane-1,3-dione (1 mmol, 0.140 g), *o*-phenylenediamine derivatives (1 mmol), and $\text{SrFe}_{12}\text{O}_{19}$ (0.02 g) were heated for 20 s under solvent-free conditions at 140 °C. Then, the aromatic aldehydes (1 mmol) were added to the mixture of reaction stirred at 140 °C for 2 min. The reaction completion was monitored by the thin layer chromatography (TLC). After completion of the reaction, the mixture was dissolved in hot EtOH, and then, the $\text{SrFe}_{12}\text{O}_{19}$ magnetic nanoparticles were easily separated from the solution by an external magnet. After a simple filtration, the solution was cooled to afford the product. The residue was purified by recrystallization from ethanol. The catalyst was subsequently washed with hot EtOH, dried under vacuum and reused for several times without significant loss of activity. The spectral data of new compounds are given below:

3,3,7-Trimethyl-2,3,4,5,10,11-hexahydro-11-[phenyl]-1*H*-dibenzo[*b,e*] [1, 4] diazepin-1-one (4b)

FT-IR (KBr) ν_{max} : 3440, 3300, 3057, 2962, 2869, 1580, and 1452 cm^{-1} ; ^1H NMR (250 MHz, DMSO- d_6) δ_{H} : 1.01 (s, 3H, CH_3), 1.05 (s, 3H, CH_3), 1.99 (s, 3H, CH_3), 2.09–2.56 (m, 4H, 2 CH_2), 3.44 and 4.36 (dt, $^2J = 5$, 1H, CH), 5.70 (d, $J = 5.25$, 1H, Ar-H), 6.08 (d, $J = 5.5$, 1H, Ar-H), 6.32 (s, 1H, N-H), 6.37 (s, 1H, Ar-H), 6.81 (d, $J = 7.75$, 1H, Ar-H), 6.98–7.10 (m, 5H, Ar-H), 8.70 (s, 1H, N-H) ppm; ^{13}C NMR (62.5 MHz, DMSO- d_6) δ_{C} : 20.61, 27.74, 29.04, 32.18, 44.53, 49.90, 56.15, 110.28, 120.40, 120.58, 121.05, 126.20, 127.69, 128.12, 128.93, 131.82, 138.74, 145.27, 155.07, 192.22 ppm; MS (m/z , %): 332 ($[\text{M}^+]$, 32), 276 (12), 255 (74), 248 (21), 234 (12), 209 (12), 132 (18), 105 (29), 91 (62), 77 (100).



Scheme 1 Synthesis of 1,5-Benzodiazepines **4a-j** using $\text{SrFe}_{12}\text{O}_{19}$ MNPs

3,3,7-Trimethyl-2,3,4,5,10,11-hexahydro-11-[(4-chloro)phenyl]-1*H*-dibenzo[*b,e*] [1,4] diazepin-1-one (**4g**)

FT-IR (KBr) ν_{max} : 3311, 3232, 3088, 2956, 2870, 1577, and 1514 cm^{-1} ; ^1H NMR (250 MHz, CDCl_3) δ_{H} : 1.05 (s, 3H, CH_3), 1.14 (s, 3H, CH_3), 2.11 (s, 3H, CH_3), 2.17–2.64 (m, 4H, 2 CH_2), 4.29 (s, 1H, CH), 5.86 (s, 1H, N–H), 6.23 (s, 1H, NH), 6.29 (s, 1H, Ar–H), 6.53–6.59 (2d, $J=7.5$, 2H, Ar–H), 7.01 (d, $J=8$, 1H, Ar–H), 7.08 (d, $J=8$, 1H, Ar–H) ppm; ^{13}C NMR (62.5 MHz, CDCl_3) δ_{C} : 20.48, 27.68, 28.83, 32.32, 46.59, 49.69, 57.38, 111.04, 120.32, 121.67, 121.93, 122.16, 124.89, 128.14, 128.26, 128.51, 132.11, 133.83, 136.57, 142.61, 152.71, 193.63 ppm; MS (m/z , %): 366 ($[\text{M}^+]$, 38), 255 (100), 157 (15), 112 (35), 105 (21), 75 (29).

Molecular docking method

The structures of all compounds were designed by the MarvinSketch software (version 6.2.2). Then, the structures were optimized with the molecular mechanic method (MM+ force field) by the HyperChem software. Also, the 3-D structure of gamma-aminobutyric acid (GABA) receptor (PDB ID: 4cof) was retrieved from the protein data bank (www.pdb.org). The water molecules and other ligands were removed from the GABA receptor before docking. CastP server (<http://sts.bioengr.uic.edu/castp/>) and FTsite server (<http://ftsitesite.bu.edu/cite>) were used for the validation of the receptor pocket [39] and determination of the ligand binding site [40], respectively. The required charge and hydrogens were added to the docking system. The docking simulation was performed using the Lamarckian Genetic Algorithm (LGA) method by the Autodock Tools 4.2 to investigate the blocking effects of **4a-j** compounds on the gamma-aminobutyric acid (GABA) receptor. The X, Y, and Z centers of the grid box were set to 6.142, –4.343, and 147.942, respectively. Furthermore, the number of points in each dimension was adjusted to X: 86, Y: 98, and Z: 50 with the spacing of

0.3750 Å. The number of docking independent runs was set to 50 with the step sizes of 0.2 Å and 5°. Among the final docked conformations of each compound, the conformation with the lowest Gibbs free energy was selected for further study. Also, the hydrogen bonds and hydrophobic interactions between different studied compounds and the GABA receptor were evaluated and represented schematically by LigPlot+ software v 1.4. The docked compounds were ranked based on the lowest binding energy, number, and length of hydrogen bonds. Some bioactivity properties, such as log P and ligand efficiency were also calculated.

Results and discussion

Application of $\text{SrFe}_{12}\text{O}_{19}$ nanoparticles in the synthesis of 1,5-benzodiazepines

The role of the $\text{SrFe}_{12}\text{O}_{19}$ magnetic nanoparticles, as nanocatalysts, for the synthesis of 4-substituted-1,5-benzodiazepines **4a-j** was investigated by the three-component domino condensation of 4,4-dimethylcyclohexane-1,3-dione **1**, *o*-phenylenediamine derivatives **2a-b**, and aromatic aldehydes **3a-h** under solvent-free conditions at 140 °C (Scheme 1).

At first, the reaction conditions were optimized. Table 1 reports the reaction times and yields under various

Table 1 The optimization of reaction condition for the synthesis of 1,5-Benzodiazepine **4f**

Entry	Catalyst	Solvent	Condition	Time	Yield (%)
1	$\text{SrFe}_{12}\text{O}_{19}$	–	r.t.	N.R.	–
2	$\text{SrFe}_{12}\text{O}_{19}$	–	120 °C	1 h	80
3	$\text{SrFe}_{12}\text{O}_{19}$	–	140 °C	140 s	90
4	–	–	140 °C	6 h	–
5	$\text{SrFe}_{12}\text{O}_{19}$	H ₂ O	Reflux	10 h	trace
6	$\text{SrFe}_{12}\text{O}_{19}$	EtOH	Reflux	6 h	65

Table 2 Synthesis of 1,5-Benzodiazepine products 4a-j in the presence of SrFe₁₂O₁₉ MNPs

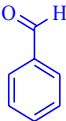
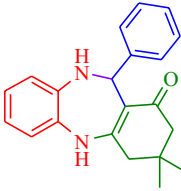
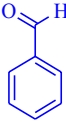
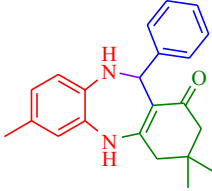
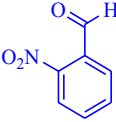
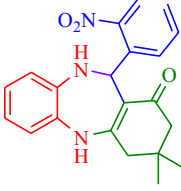
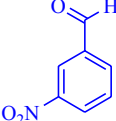
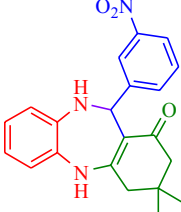
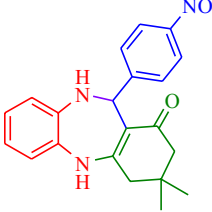
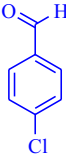
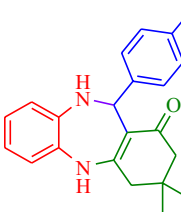
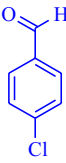
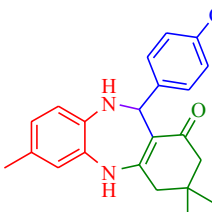
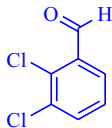
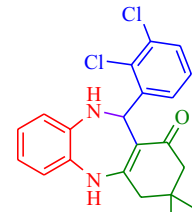
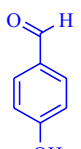
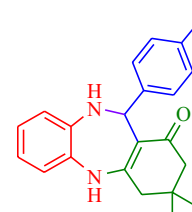
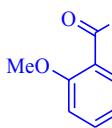
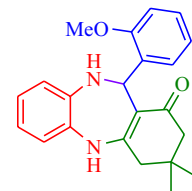
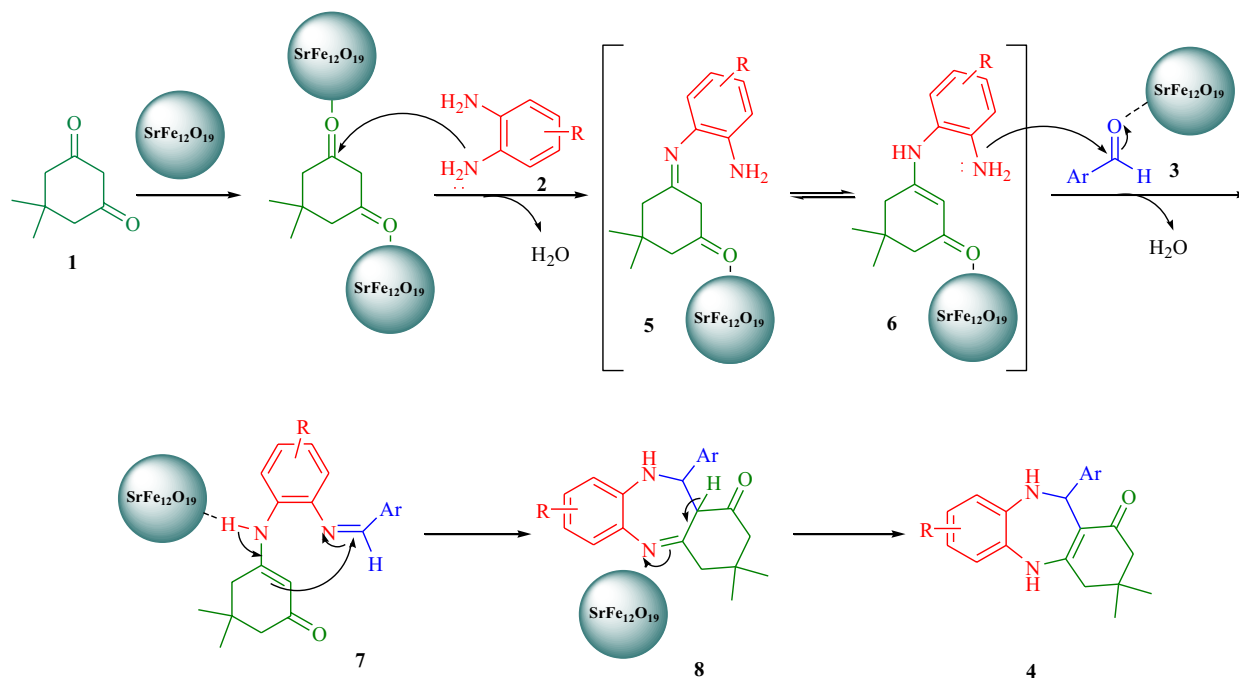
Entry	No.	R	Aldehydes	Products	Yield (%)	m.p. (°C)	m.p. [Ref.]
1	4a	H			85	247–249	251–252 [41]
2	4b	CH ₃			89	252*	New
3	4c	H			94	120–121	115–117 [42]
4	4d	H			92	194–196	195–197 [41]
5	4e	H			94	275–276	280–282 [15]
6	4f	H			90	245–247	251–253 [41]
7	4g	CH ₃			96	240–242	New

Table 2 (continued)

Entry	No.	R	Aldehydes	Products	Yield (%)	m.p. (°C)	m.p. [Ref.]
8	4h	H			75	255	256–258 [23]
9	4i	H			78	230	225 [42]
10	4j	H			87	220	217–218 [42]

4,4-Dimethyl cyclohexane-1,3-dione (1 mmol, 0.140 g), *o*-phenylenediamine derivatives (1 mmol), and SrFe₁₂O₁₉ (0.02 g) was heated for 20 s under solvent-free conditions at 140 °C. Then, the aromatic aldehydes (1 mmol) were added to the mixture of reaction stirred at 140 °C for 2 min



Scheme 2 Proposed mechanism for the synthesis of 1,5-Benzodiazepines

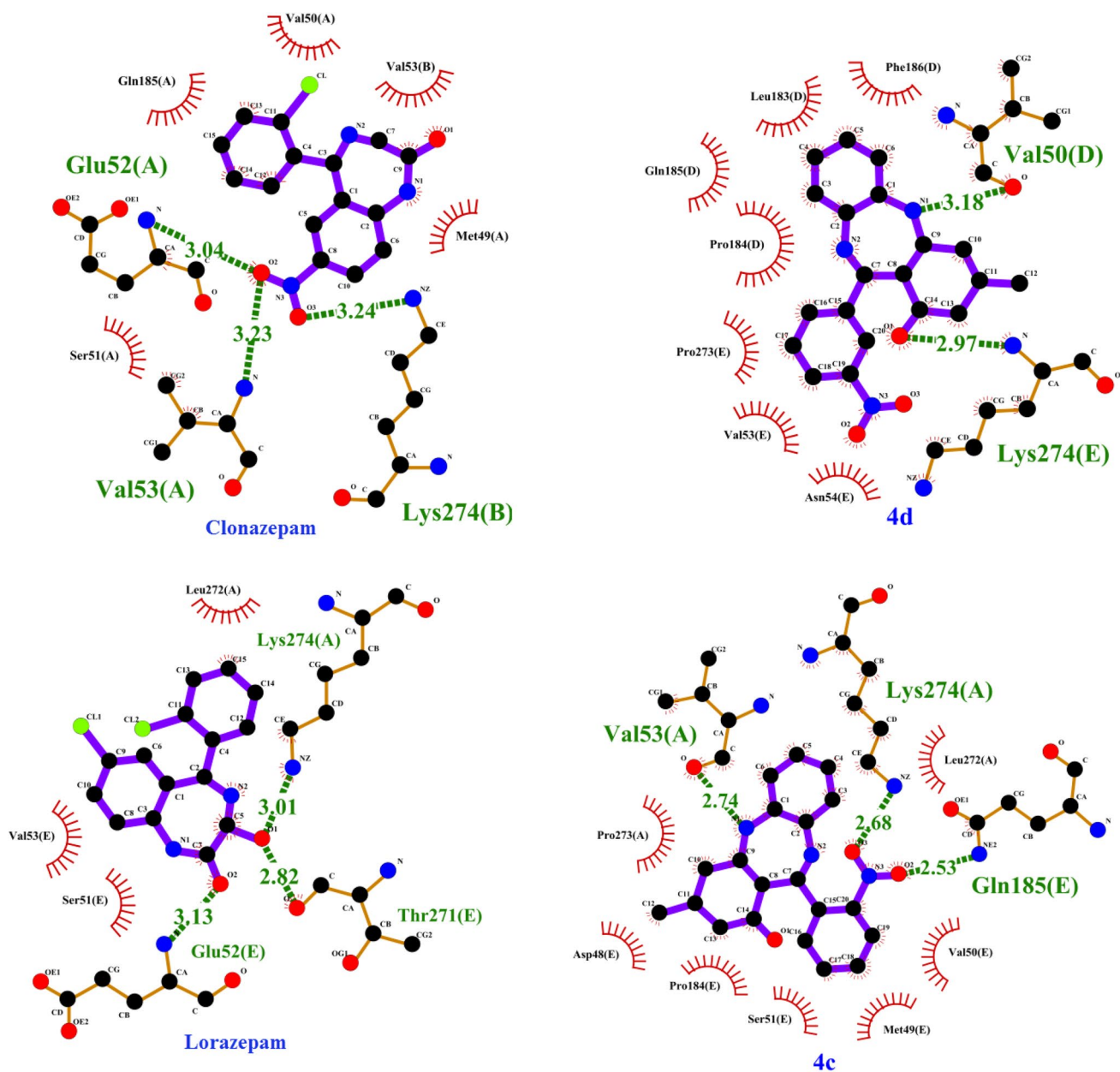


Fig. 1 2D representation of hydrogen bonds and hydrophobic interactions between the synthesized compounds and GABA receptor. The docking was performed by the AutoDock Tools, and the results were analyzed by the LigPlot⁺ software. The green dashed lines

denote the hydrogen bonds in Å. The compounds 4c and 4d, shown here, have higher binding affinities among all the studied compounds. Lysine274, Valine53, Valine50, and Asparagine54 residues are the main amino acids contributing in the interactions

conditions. Accordingly, the best result was obtained after 140 s under solvent-free conditions. In the absence of the catalyst under solvent-free conditions, the yield of the desired product was trace even after 6 h (Table 1, entry 4). These optimized reaction conditions were extended to a range of *o*-phenyldiamines, 4,4-dimethyl cyclohexane-1,3-dione, and aromatic aldehydes in the presence of the SrFe₁₂O₁₉ MNPs under solvent-free conditions at 140 °C.

The new products were characterized by their melting points and the usual spectroscopic techniques, i.e., IR, ¹H NMR, ¹³C NMR, and MS spectroscopies. The melting points of the synthesized products were compared with those available in the literature (Table 2). The scope of reaction was tested by the use of various benzaldehydes bearing either electron releasing or electron withdrawing substituents. The yields of products 4a–4g were high showing the positive role of electron withdrawing substituents. While electron

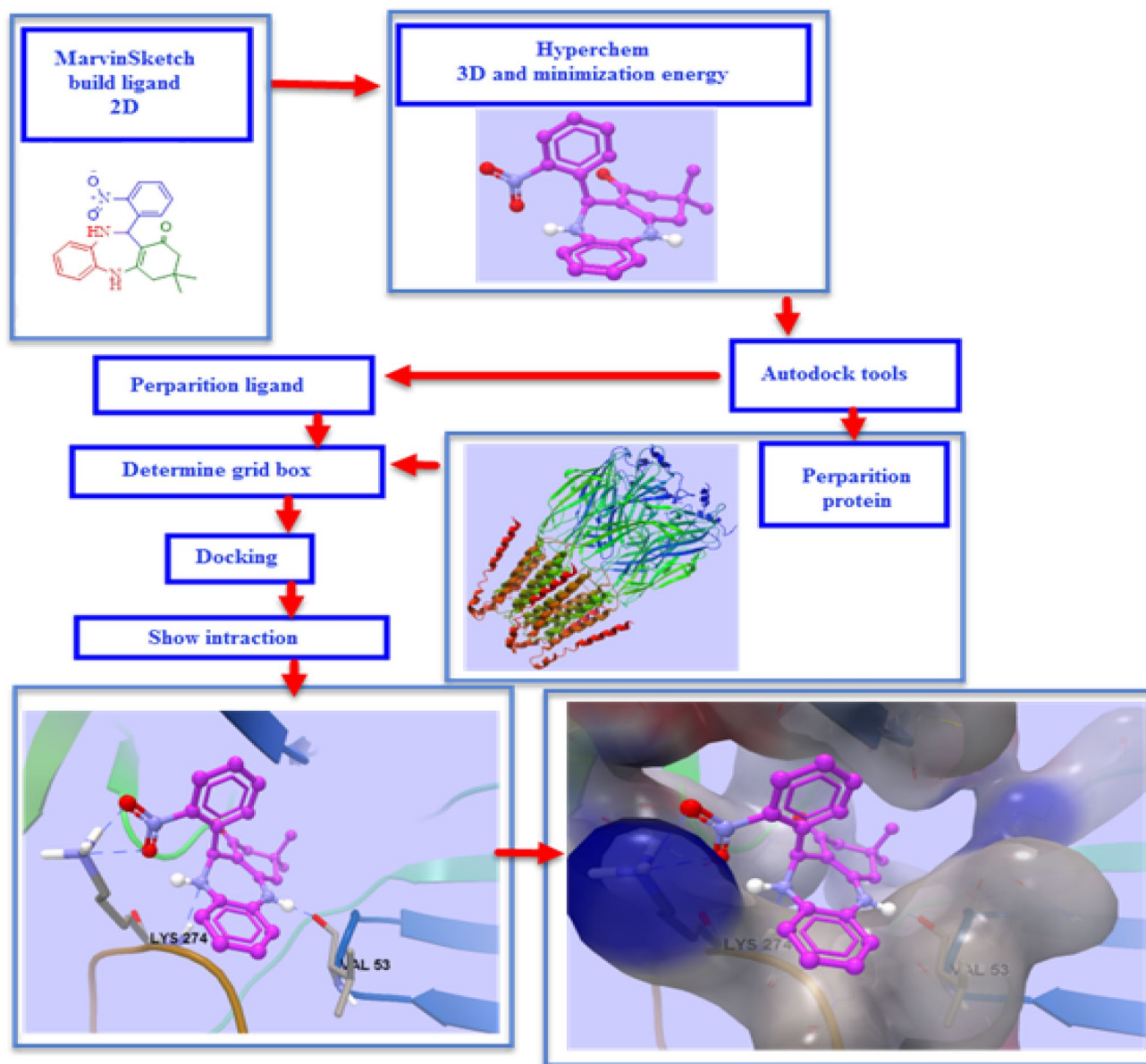


Fig. 2 Schematic diagram of the docking procedure in this study. At first, the compounds were designed by MarvinSketch and then optimized by Hyperchem. Then, the ligands and protein were prepared

using AutoDock Tools, and the system was finally docked after setting the grid box. A 3-D view of the interactions between 4c and the GABA receptor is shown using the CLC drug discovery

releasing groups of OH and OMe led to the significant drop in the yield of **4i-j**. The drop in the yield of **4h** may be as a result of steric hindrance of 2-Cl group.

A plausible mechanism for the studied reaction is shown in Scheme 2. The $\text{SrFe}_{12}\text{O}_{19}$ MNPs plays a significant role in the acceleration of the reaction. At first, in the presence of $\text{SrFe}_{12}\text{O}_{19}$, the intermediate 5, which is produced from the reaction of 4,4-dimethyl cyclohexane-1,3-dione 1 and *o*-phenylenediamines 2, was isomerized to the more stable enamine

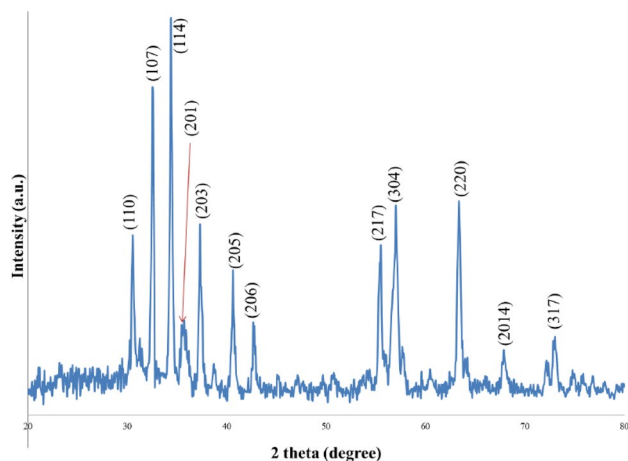
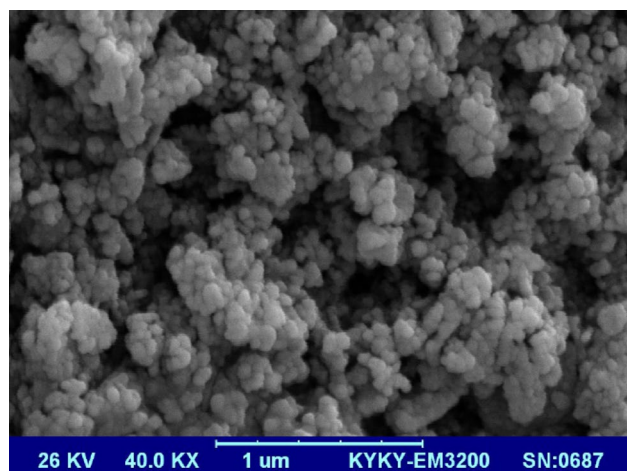
intermediate 6. Condensation of the enamine 6 and aldehyde 3 is accomplished to produce the imine 7, which affords the desired final 1,5-benzodiazepines 4 after the intramolecular Mannich reaction and isomerization.

Molecular docking analysis

Gamma-aminobutyric acid type A (GABAA) receptors, which mediate neuronal inhibition, are parts of the

Table 3 Calculated binding energy, electrostatic energy, ligand efficiency and log P for the compounds docked

Component	Binding energy (Kcal/mol)	Electrostatic energy	Ligand efficiency	Log P
Clonazepam	-8.01	-1.23	-0.35	2.79
Lorazepam	-7.43	-0.08	-0.36	3.17
4a	-8.01	-0.08	-0.33	4.50
4b	-8.08	-0.09	-0.32	4.97
4c	-9.2	-1.34	-0.34	3.51
4d	-9.08	-0.26	-0.34	3.51
4e	-6.61	-0.97	-0.24	4.45
4f	-6.6	-0.04	-0.26	4.18
4g	-6.58	-0.14	-0.25	5.49
4h	-7.1	-0.03	-0.27	4.78
4i	-6.58	-0.27	-0.26	4.22
4j	-6.46	-0.09	-0.25	3.41

**Fig. 3** XRD pattern of SrFe₁₂O₁₉ nanoparticles**Fig. 4** SEM image of SrFe₁₂O₁₉ nanoparticles

neurotransmitter ligand-gated ion channels. The effects of GABA on the GABA_A receptors are known to be modulated by a range of therapeutically necessary drugs, such as anesthetics, barbiturates, and benzodiazepines (BZs). Before docking the synthesized benzodiazepine compounds, we need to identify the binding sites of BZs, and therefore, the clonazepam and lorazepam drugs were first docked with the GABA receptor. Accordingly, in the binding site of BZs, Lys274 in the γ subunit and Val53, Val50, Asn54, Glu52, and Thr271 in the α subunit were found to have the major role. These sites are important in the molecular docking studies and de novo drug design [43].

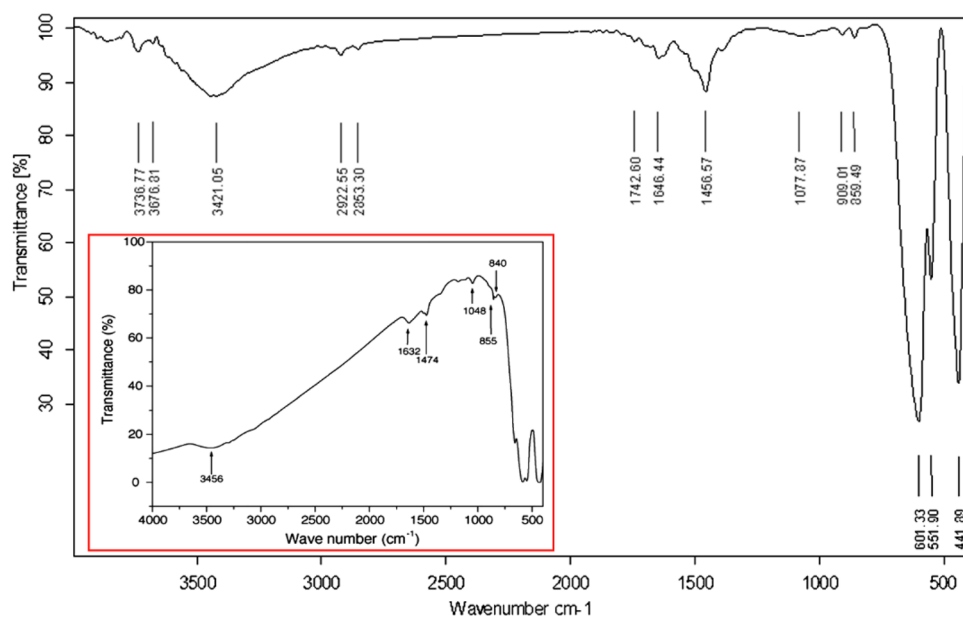
After finding the binding sites of BZs, each compound was docked with the GABA receptor. Figure 1 shows the docking mode of the compounds with the GABA receptor. The best docking score (the lowest ΔG) was selected among thirty docked compounds. The obtained results revealed that the docked compounds can competitively occupy the binding pocket of the BZs. Some polar residues in the binding site of the BZs, including Asp48, Val50, Ser51, Glu52, Val53, Gln185, and Lys274, interact with the studied compounds in the form of hydrogen bonds or electrostatic interactions (Fig. 1). The docking binding energy of -9.2 kcal/mol was selected among ten docked compounds. Figure 1 shows the interaction diagram for the compounds 4c and 4d with the α and γ subunits of the GABA receptor. The compounds were embedded into the binding site of BZs in the GABA receptor. The seventeen residues surrounding the BZs binding site, including the Asp48, Met49, Val50, Ser51, Glu52, Val53, Asn54, Leu183, Pro184, Gln185, Phe186, Thr220, Gln270, Thr271, Leu272, Pro273, and Lys274 significantly contribute in the stabilization of the 4c-GABA receptor complex. Lys274 and val53, the crucial residues in the binding pocket of the BZs, are partly responsible for the binding of the BZs to the GABA receptor (Fig. 2). The compounds 4c and 4d showed higher binding affinity to the GABA receptor, and therefore, they have more inhibitive effect than the other studied compounds.

Also, the compounds 4c and 4d establish 3 and 2 hydrogen bonds, respectively. Moreover, the average length the hydrogen bonds length in 4c is shorter, and therefore, 4c is more strongly bound to the receptor. The estimated values of binding energy, electrostatic energy, and ligand efficiency for the compounds – receptor complex are listed in Table 3.

Suggestion using drugs

The BZs that can cross the blood brain barrier (BBB) are effective. The evaluation of the brain–blood crossing in vitro is difficult. Therefore, we used an alternative method based on log P (fat-soluble factor). The values of log P (lipophilicity), indicating the biological activity of small molecules, were obtained using the Marvin software [43]. A compound

Fig. 5 FT-IR spectrum of the $\text{SrFe}_{12}\text{O}_{19}$ nanoparticles, inset: FT-IR of the same compounds obtained by Jean et al. [45]



can cross the BBB when its log P is at least 2.0 [44]. The values of log P for all selected compounds are between 3.26 and 5.49 (Table 3). Accordingly, all of the synthesized compounds have log P values higher than 2, which is necessary for their sufficient entry into the brain. Also, the obtained log P values of the studied compounds are higher than those of clonazepam and lorazepam.

Characterization of the $\text{SrFe}_{12}\text{O}_{19}$ nanoparticles

The X-ray diffraction pattern of the prepared $\text{SrFe}_{12}\text{O}_{19}$ MNPs with a magnetoplumbite structure is displayed in Fig. 3. The XRD pattern showed twelve characteristic peaks including $2\theta = 30.55^\circ, 32.53^\circ, 34.39^\circ, 35.47^\circ, 37.33^\circ, 40.63^\circ, 42.67^\circ, 55.51^\circ, 57.01^\circ, 63.37^\circ, 67.87^\circ,$ and 72.85° which can be indexed to the (110), (107), (114), (201), (203), (205), (206), (217), (304), (220), (204), and (317) lattice planes, respectively. The results definitely confirm the

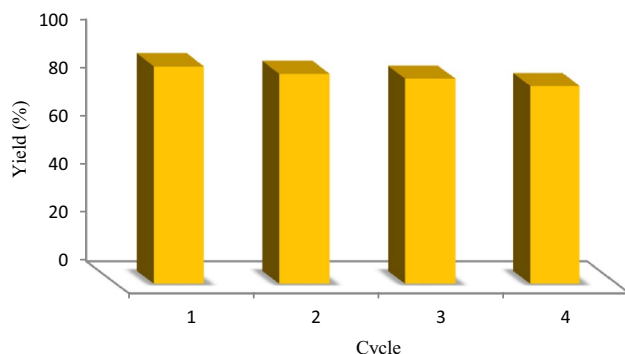


Fig. 6 Reusability of $\text{SrFe}_{12}\text{O}_{19}$ MNPs for the synthesis of compound **4f**

successful formation of $\text{SrFe}_{12}\text{O}_{19}$ nanoparticles. According to the SEM image, the $\text{SrFe}_{12}\text{O}_{19}$ particles are spherical with the average size of about 70 nm (Fig. 4).

FT-IR of $\text{SrFe}_{12}\text{O}_{19}$ MNPs (Fig. 5) shows a broad band around 3421 cm^{-1} related to the stretching vibration of the adsorbed H_2O molecules; the band corresponding to the bending vibrations of H_2O is seen at 1646 cm^{-1} . The spectrum displays two weak bands at 840 and 1077 cm^{-1} corresponding to the vibrations of nitrate groups (remaining from the initial reactant). The large bands at 1456 and 859 cm^{-1} could be assigned to the carboxylate vibration ($-\text{COO}-$) from the used organic acids. The sharp bands at $441, 551, 601\text{ cm}^{-1}$ are related to the $\text{SrFe}_{12}\text{O}_{19}$. All these observations were in agreement with the consequences obtained by Jean et al. [45].

We investigated the recovery and reusability of the $\text{SrFe}_{12}\text{O}_{19}$ nanocatalyst for the production of the compound **4f** as a typical example. As shown in Fig. 6, the catalyst was recycled four times without significant loss of activity. The yields of the first four successive runs were 90, 87, 85, and 82%, respectively.

Conclusion

The $\text{SrFe}_{12}\text{O}_{19}$ magnetic nanoparticles [46–49] can be used as green solid acid nanocatalysts in our facile and efficient developed approach for the synthesis of 4-substituted-1,5-benzodiazepines under solvent-free conditions. Several advantages of this approach include its operational simplicity, excellent product yields, non-chromatographic purification, short reaction time, simple and easy work-up procedure, and environmentally benign conditions.

The results showed that the SrFe₁₂O₁₉ nanoparticles are effective, recoverable, and reusable catalysts. They are easily separated from the reaction mixture by the use of an external magnet. The interaction parameters between the obtained products and the GABA receptor were evaluated by LigPlot⁺ software v.1.4. The electrostatic energy, ligand efficiency, log P, and total binding energy of the compounds with the receptor were also calculated. The log P values of the synthesized compounds, which were greater than 2, were higher than those of the clonazepam and lorazepam.

Supplementary Information The online version of this article (<https://doi.org/10.1007/s13738-021-02163-6>) contains supplementary material, which is available to authorized users.

Acknowledgment We gratefully acknowledge the financial support from the Research Council of Alzahra University and the University of Tehran.

References

1. L. Leggio, G.A. Kenna, R.M. Swift, *Prog. Neuropsychopharmacol. Biol. Psychiatry* **32**, 1106 (2008)
2. K. Bhagat, A. Singh, S. Dhiman, J.V. Singh, R. Kaur, G. Kaur, H.K. Gulati, P. Singh, R. Kumar, R. Salwan, *Med. Chem. Res.* **28**, 2200 (2019)
3. N. Arora, P. Dhiman, S. Kumar, G. Singh, V. Monga, *Bioorg. Chem.* **97**, 103668 (2020)
4. M.N. Timofeeva, E.A. Petrova, E.A. Mel'gunova, A. Gil, M.A. Vicente, V.N. Panchenko, *React. Kinet. Mech. Catal.* **127**, 41 (2019)
5. W.-B. Yi, C. Cai, *J. Fluorine Chem.* **130**, 1054 (2009)
6. M. Kodomari, T. Noguchi, T. Aoyama, *Synth. Commun.* **34**, 1783 (2004)
7. B.E. Leonard, *Hum. Psychopharmacol. Clin. Exp.* **14**, 125 (1999)
8. A.M. Holbrook, R. Crowther, A. Lotter, C. Cheng, D. King, *Can. Med. Assoc. J.* **162**, 225 (2000)
9. J. Xu, G. Zuo, W.L. Chan, *Heteroat. Chem.* **12**, 636 (2001)
10. H. Uchida, T. Suzuki, D.C. Mamo, B.H. Mulsant, T. Kikuchi, H. Takeuchi, M. Tomita, K. Watanabe, G. Yagi, H. Kashima, *J. Anxiety Disord.* **23**, 477 (2009)
11. X.-Q. Pan, J.-P. Zou, Z.-H. Huang, W. Zhang, *Tetrahedron Lett.* **49**, 5302 (2008)
12. M. Aversa, A. Ferlazzo, P. Giannetto, F. Kohnke, *Synthesis.* **1986**, 230 (1986)
13. A. Chimirri, S. Grasso, R. Ottanà, G. Romeo, M. Zappalà, *J. Heterocycl. Chem.* **27**, 371 (1990)
14. J.J.V. Eynde, A. Mayence, A. Maquestiau, E. Anders, *Bull. Soc. Chim. Belg.* **101**, 801 (1992)
15. N.N. Kolos, E.N. Yurchenko, V.D. Orlov, S.V. Shishkina, O.V. Shishkin, *Chem. Heterocycl. Compd.* **40**, 1550 (2004)
16. Y. Wang, M.-S. Tu, F. Shi, S.-J. Tu, *Adv. Synth. Catal.* **356**, 2009 (2014)
17. X.-T. Zhu, J.-Y. Liu, B. Jiang, S.-J. Tu, *J. Heterocycl. Chem.* **52**, 92 (2015)
18. J. Dai-II, C. Tae-wonchoi, K. Yun-Young, K. In-Shik, P. You-Mi, L. Yong-Gyun, J. Doo-Hee, *Synth. Commun.* **29**, 1941 (1999)
19. J.A. Herbert, H. Suschitzky, *J. Chem. Soc. Perkin Trans.* **1**, 2657 (1974)
20. H.R. Morales, A. Bulbarela, R. Contreras, *Heterocycles.* **24**, 135 (1986)
21. R. Kaoua, B. Nedjar-Kolli, T. Roisnel, Y. Le Gal, D. Lorcy, *Tetrahedron.* **69**, 4636 (2013)
22. R. Varala, R. Enugala, S. Nuvula, S.R. Adapa, *Synlett.* **2006**, 1009 (2006)
23. H. Naeimi, H. Foroughi, *Chin. J. Catal.* **36**, 734 (2015)
24. G. Sabitha, G. Reddy, K.B. Reddy, N.M. Reddy, J. Yadav, *Adv. Synth. Catal.* **346**, 921 (2004)
25. M.A. Pasha, V.P. Jayashankara, *Heterocycles.* **68**, 1017 (2006)
26. R.G. Jacob, C.S. Radatz, M.B. Rodrigues, D. Alves, G. Perin, E.J. Lenardao, L. Savegnago, *Heteroat. Chem.* **22**, 180 (2011)
27. A. Maleki, *Tetrahedron.* **68**, 7827 (2012)
28. M.R. Shushizadeh, N. Dalband, *Jundishapur J. Nat. Pharm. Prod.* **7**, 61 (2012)
29. H. Naeimi, H. Foroughi, *New J. Chem.* **39**, 1228 (2015)
30. M. Pozarentzi, J. Stephanidou-Stephanatou, C.A. Tsoleridis, *Tetrahedron Lett.* **43**, 1755 (2002)
31. M.S. Balakrishna, B. Kaboudin, *Tetrahedron Lett.* **42**, 1127 (2001)
32. T. Ahmadi, S. Bahar, G. Mohammadi Ziarani, A. Badiei, *Food Chem.* **300**, 125180 (2019)
33. T. Ahmadi, G. Mohammadi Ziarani, S. Bahar, A. Badiei, *J. Iran. Chem. Soc.* **15**, 1153 (2018)
34. M.G. Hasab, S.A. Seyyed Ebrahimi, A. Badiei, *J. Eur. Ceram. Soc.* **27**, 3637 (2007)
35. S. Alamolhoda, S.A. Seyyed Ebrahimi, A. Badiei, *J. Magn. Magn. Mater.* **303**, 69 (2006)
36. S. Alamolhoda, S.A. Seyyed Ebrahimi, A. Badiei, *Iran. Int. J. Sci.* **5**, 173 (2004)
37. G. Mohammadi Ziarani, Z. Kazemi Asl, P. Gholamzadeh, A. Badiei, M. Afshar, *Appl. Organomet. Chem.* **31**, e3830 (2017)
38. G. Mohammadi Ziarani, Z. Kazemi Asl, P. Gholamzadeh, A. Badiei, M. Afshar, *J. Sol. Gel Sci. Technol.* **85**, 103 (2018)
39. J. Dundas, Z. Ouyang, J. Tseng, A. Binkowski, Y. Turpaz, J. Liang, *Nucleic Acids Res.* **34**, W116 (2006)
40. C.-H. Ngan, D.R. Hall, B. Zerbe, L.E. Grove, D. Kozakov, S. Vajda, *Bioinformatics.* **28**, 286 (2012)
41. M.D.R. Arellano, R. Martínez, E. Cortés, *J. Heterocycl. Chem.* **19**, 321 (1982)
42. V. Hazai, T. Szabó, B. Volk, M. Milen, *Chem. Heterocycl. Compd.* **56**, 237 (2020)
43. T.C. Jacob, S.J. Moss, R. Jurd, *Nat. Rev. Neurosci.* **9**, 331 (2008)
44. P.S. Miller, A.R. Aricescu, *Nature.* **512**, 270 (2014)
45. M. Jean, V. Nachbaur, J. Bran, J.-M. Le Breton, *J. Alloys Compd.* **496**, 306 (2010)
46. Z. Kheilkordi, G. Mohammadi Ziarani, A. Badiei, *Polyhedron* **178**, 114343 (2020)
47. Z. Kheilkordi, G. Mohammadi Ziarani, S. Bahar, A. Badiei, *J. Iran. Chem. Soc.* **16**, 365 (2019)
48. Z. Kheilkordi, G. Mohammadi Ziarani, N. Lashgari, A. Badiei, *Polyhedron* **166**, 203 (2019)
49. Z. Kheilkordi, G. Mohammadi Ziarani, A. Badiei, N. Lashgari, *Sensor Lett.* **17**, 747 (2019)